

Model identification and data fusion for the purpose of the altitude control of the VTOL aerial robot

Roman Czyba * Wojciech Janusz * Grzegorz Szafranski *

* *Silesian University of Technology, 44-100 Gliwice, Poland (e-mail: roman.czyba@polsl.pl, wojciech.janusz@polsl.pl, grzegorz.szafranski@polsl.pl).*

Abstract: In this paper we focus on the problem of the altitude control for an unmanned aerial vehicle known as quadrotor. One of the requirements for the proper operation of altitude control system, are reliable estimates of the UAV altitude and vertical velocity. In this paper altitude and vertical speed estimation algorithm in a form of the Kalman filter is presented which makes use of the ultrasonic range finder and accelerometer. On the basis of the estimates, the nonlinear Hammerstein-Wiener model of the velocity and parametric model of altitude are constructed. Next, the model of the quadrotor vertical movement is used in a process of cascade control system design. Finally, the verification of the controllers has been performed on the hardware platform, and the performance of the altitude controller has been examined.

Keywords: State estimation, Velocity control, Autonomous vehicles, Parameter identification, Identification algorithms

1. INTRODUCTION

In several recent years, there has been a great boom on many kinds of the unmanned aerial vehicles (UAVs), especially vertical take-off and landing platforms with multirotor actuators. One of the main reasons for the gain of their popularity, is the ability to perform vertical take-off and landing tasks. It allows to operate indoors and/or with low linear speeds making it for example an useful tool for surveillance missions. One of the problem which arises during the development of this kind of platform, is how to ensure its ability to maintain desired values of the attitude/altitude because of the fact, that these object are structurally unstable. Although the development of Micro Electro- Mechanical Systems gave the opportunity to design very small in size and powerful electronic circuits that consist of miniature sensors and high performance microprocessors which can be used in a character of control units Bristeau et al. (2011), there still exists problem of the measurements and the methodology of control system prototyping. Modern control theory includes variety of methods suitable for the design of control systems, but in order to employ them, one needs to use some kind of the model describing plant dynamics. While building model of VTOL robot we encounter many issues related to the topics of the state estimation and mathematical modeling.

This paper address the topics of state estimation/ identification and altitude control in a connection to VTOL objects. At the beginning nonlinear VTOL model is presented, it is separated into two parts, rigid body dynamics and a part describing propulsion system. Then measurement instruments mounted on a experimental platform will be described together with the problems related to each of these instruments. Further, proposed estimation al-

gorithm, consisting of a nonlinear filter and Kalman Filter will be described. State estimates obtained from the filter, will be used as a reference values in the process of system identification, in a character of a model, Hammerstein-Wiener model is employed. In order to validate the identification results, performance of the control loop designed using the simulation model will be checked. In this way, it will be possible to prove, that constructed model can be efficiently used in the process of control scheme design.

2. VERTICAL MOVEMENT MODEL

There is significant amount of literature dedicated to quadrotors, where the model of platform dynamics is used (Bouabdallah et al. (2004), Bouabdallah (2007), Castillo et al. (2005), Nonami et al. (2010), Tayebi and McGilvray (2006), Valavanis (2007)). The dynamic model is derived using Euler-Lagrange formalism under the following assumptions: the frame structure is rigid, the structure is symmetrical, the centre of gravity (CoG) and the body fixed frame origin are assumed to coincide, the propellers are rigid. Taking these into account, the quadrotor mathematical model can be divided into two subsystems: rigid body model and propulsion with aerodynamic phenomena occurring during quadrotor operation Fig. 1.

2.1 Rigid body model

The detailed derivation of equations given below can be found in Castillo et al. (2005), Tayebi and McGilvray (2006), Bouabdallah et al. (2004), Bouabdallah (2007). The quadrotor dynamic model with x, y, z motions as a consequence of a pitch, roll and yaw rotation is as follows:

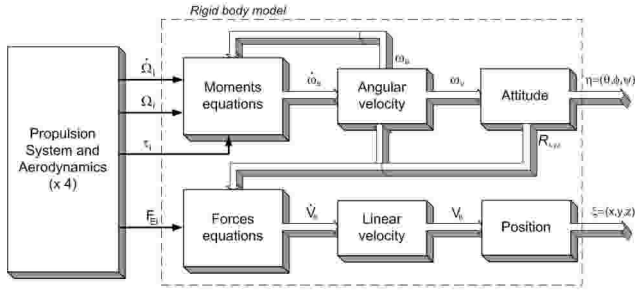


Fig. 1. Block diagram of system dynamics

$$\begin{aligned}
 \ddot{\phi} &= 1/I_{xx}((I_{yy} - I_{zz})\dot{\psi}\dot{\theta} + T_{\phi}) \\
 \ddot{\theta} &= 1/I_{yy}((I_{zz} - I_{xx})\dot{\psi}\dot{\phi} + T_{\theta}) \\
 \ddot{\psi} &= 1/I_{zz}((I_{xx} - I_{yy})\dot{\theta}\dot{\phi} + T_{\psi}) \\
 \ddot{x} &= f_g/m(\sin(\psi)\sin(\phi) + \cos(\psi)\sin(\theta)\cos(\phi)) \\
 \ddot{y} &= f_g/m(\sin(\psi)\sin(\theta)\cos(\phi) - \cos(\psi)\sin(\phi)) \\
 \ddot{z} &= f_g/m(\cos(\theta)\cos(\phi)) - g
 \end{aligned} \quad (1)$$

where: ϕ, θ, ψ - the Euler angles, x, y, z - the position of the centre of quadrotor mass with respect to a fixed reference frame, I_{xx}, I_{yy}, I_{zz} - inertia moments, $T_{\phi}, T_{\theta}, T_{\psi}$ - torques consist of the difference in the action of the thrust forces for each pair and the gyroscopic effect, m - platform's mass, g - Earth's gravity acceleration, f_g - total thrust coming from the rotors. The total thrust is given as:

$$f_g = F_1 + F_2 + F_3 + F_4 \quad (2)$$

It is important to notice that the F_i contains the model of propulsion system, aerodynamic drag and environmental disturbances.

2.2 Propulsion system

In general, rotary-wing aircraft have no lifting surface. All the thrust force is generated thanks to the propulsion system, which in most cases consists of the BLDC motor and a propeller, which is mounted without any gearbox directly on the motor shaft. Brushless DC motor dynamics can be modelled as follows. From basic physics principles the electrical equation of the system has the following form:

$$u_m - i_m R_m - L_m \frac{di_m}{dt} - e_m = 0, \quad e_m = k_{emf} \Omega \quad (3)$$

where: u_m - voltage applied to the motor, i_m - armature current, R_m - motor winding resistance, L_m - inductance, e_m - back electromotive force, k_{emf} - motor electrical constant, Ω - shaft velocity. Motor torque T_m is proportional to the armature current i_m . The load has an opposing torque T_0 . The mechanical equation can be expressed as follows:

$$J\dot{\Omega} - T_m - T_0 - B\Omega = 0, \quad T_m = k_m i_m \quad (4)$$

where: J - rotor and propeller inertia, B - viscous friction coefficient, k_m - torque constant. The torque produced by the motor drives the propeller with the same angular velocity because of the direct connection.

2.3 Rotor in vertical flight: momentum theory

The principle of the thrust generation process can be fully explained by the approach commonly referred to as momentum theory (Seddon (1990), Leishman (2006)). Quadrotor must operate in a variety of flight regimes. Our considerations are limited to the vertical movement, which includes hover, climb and descent. In hover or axial flight, the flow is axisymmetric and the flow through the rotor is either upward or downward. The relationship between the rotor thrust T and the induced velocity V_i at the rotor disk in hover is:

$$V_h = V_i = \sqrt{\frac{T}{2\rho A}} \quad (5)$$

where: V_h - rotor inflow velocity in hover, ρ - air density, A - disc area of a rotor. For the climbing rotor the relationship is as follows:

$$T = 2\rho A(V_c + V_i)V_i \quad (6)$$

where: V_c - vertical rotor velocity. In the climb the induced velocity V_i is given by the ratio:

$$\frac{V_i}{V_h} = -\left(\frac{V_c}{2V_h}\right) + \sqrt{\left(\frac{V_c}{2V_h}\right)^2 + 1}, \quad V_c > 0 \quad (7)$$

This is normal working state of the rotor with hover being lower limit. For the axial descent the above model cannot be used, and it is required to consider two following cases. First,

$$\frac{V_i}{V_h} = -\left(\frac{V_c}{2V_h}\right) - \sqrt{\left(\frac{V_c}{2V_h}\right)^2 - 1}, \quad V_c \leq 2V_h \quad (8)$$

The rotor is extracting power from the airstream and this operating condition is known as the windmill brake state, because the rotor decreases or brakes the velocity of the flow.

Second case, it is the region between hover and windmill state. When momentum theory is invalid because the flow can take on two possible directions and a well-defined slipstream ceases to exist. Unfortunately descending flight accentuates interactions of the tip vortices with other blades and so the flow becomes rather unsteady and turbulent, and experimental measurements of rotor thrust and power are difficult to make. In this case the curve of V_i is not analytically predictable. The experimental estimates can be used to find the best approximation for induced velocity at any rate of descent. Many authors, including Young and Johnson, suggest a linear approximation (Leishman (2006), Seddon (1990)).

After analysing the rigid body model and propulsion system with its aerodynamics, the remarks are as follows:

Remark 1. The relative order of quadrotor model is equal four, which claims about the complexity of the quadrotor dynamics.

Remark 2. Taking into account different phases of vertical flight (climb, descent and hover) the nonlinearities make difficulties in the synthesis of the control system.

Remark 3. Due to the problems with the parameters determination of the phenomenological model, an identification techniques are recommended.

3. STATE ESTIMATION AND MEASUREMENT FILTRATION

Let us describe at the beginning the measurement system in the sense of its error/noise characteristics. We assume that VTOL platform is equipped with the following instruments:

- Accelerometer which measures acceleration along z-axis of VTOL platform,
- Ultrasonic range finder which is pointing downwards along VTOL z-axis.

Details of each of the instruments will be shortly discussed in separate paragraphs.

3.1 Accelerometer

The triaxial accelerometer has been used for the altitude estimation algorithm. It has been a part of a triaxial inertial sensor with magnetometer ADIS 16400. The range of the accelerometer is about $\pm 18g$. Factory calibration coefficients allow to obtain for each sensor its own dynamic compensation in order to provide accurate sensor measurements over a wide range of temperatures ($-40^\circ C$ to $+85^\circ C$). The misalignment of the sensor axis is about 0.2 degrees. Nonlinearity of the sensor is a 0.1 % of a full scale while the sensor output noise is less than 9mg rms.

One of the basic issues related to the acceleration measurement, is high vulnerability of the measurement to the VTOL frame vibrations which results in a high variance noise. At the same time, assumption about zero mean value of this noise is too optimistic, which can result in a drift, when one would like to obtain a linear velocity based on the integration of the accelerometer measurements. In a further part of the article, accelerometer measurements will have compensated gravitational acceleration component, so in a case when VTOL stays on the ground readings will be equal to 0 instead of 1g.

3.2 Ultrasonic sensor

An ultrasonic sensor is a distance measuring unit which consists of an integrated ultrasonic waves transmitter, receiver and signal processing circuit. The sensor XL-EZ0 that has been used in the autopilot electronics detects object from 20 to more than 700 centimeters with a 1 centimeter resolution. Sonar series is capable to operate in a variable conditions such as temperature, voltage and acoustic or electrical noise changes. It has been provided with an auto-calibration function. Sensor operates at 42kHz frequency and measurements are available every 100 milliseconds.

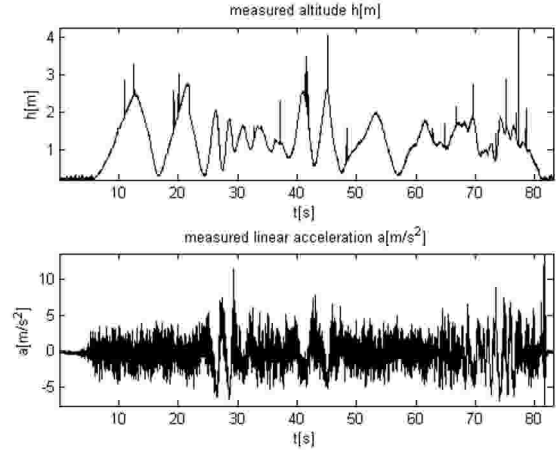


Fig. 2. Measurements obtained during the identification experiment

In case of the ultrasonic sensor, the main problem is related with reflections of the beam emitted by the sensor itself, these reflections results in a high amplitude pulses in the altitude readings. This behavior is very undesirable especially when such measurement is used as feedback signal in control loop, attempt of overcoming this problem by use of downpass filter introduce large phase lag in the control loop. Another issue in case of ultrasonic sensor is its short range.

On Figure 2 measurements from identification experiment are depicted. One can see large amplitude noise in acceleration measurements and pulse errors in the ultrasonic measurement data.

State estimation will be carried out in two steps, at the beginning nonlinear filtering of ultrasonic sensor readings takes place, then in a role of the state estimator Kalman filter will be used.

3.3 Ultrasonic sensor measurements filter

In the first step it is desirable to attenuate spike errors present in ultrasonic sensor measurements. These spikes are a result of the beam reflections, such reflection can occur when emitted beam for example hits walls when flight takes place indoor or leaves when VTOL is starting from the ground in the outdoor environment. Ultrasonic sensor measurements are filtered with use of a nonlinear filter Szafranski et al. (2013). Task of this nonlinear filter is to limit the rate of change of the signal coming from the ultrasonic sensor. With this approach it is possible to remove high amplitude pulses that are present in the measurement. This filter consists of a saturation, gain and an integral, these elements are enfolded by a negative feedback loop. Rate of change limiter can be written using a nonlinear differential equation (9) where e is a difference between actual ultrasonic sensor readings and the output of rate of change limiter.

$$\dot{h}_{US}^F = k_{rl} \text{sat}_B(e) = \begin{cases} k_{rl} B_{rl}; & e > B_{rl} \\ k_{rl} e; & |e| \leq B_{rl} \\ -k_{rl} B_{rl}; & e < -B_{rl} \end{cases} \quad (9)$$

Gain inside the filter will be denoted as k_{rl} , saturation limits will be denoted as B_{rl} . From the equation (9), it is clear, that the derivative of the output is bounded by the values $k_{rl}B_{rl}$ and $-k_{rl}B_{rl}$. At the same time, when signal e is not affected by the saturation function (because of its low absolute value), whole filter acts as a first order lag. By use of sufficiently high gain k_{rl} and adequately to it chosen saturation level B_{rl} , it is possible to obtain low values of phase lag between signal before and after filtering, while being able to filter out the high amplitude pulses found in ultrasonic sensor readings.

3.4 Kalman Filtering

In order to implement Kalman filter, the following plant model was assumed (10).

$$\begin{aligned}\dot{b}_{acc} &= \eta_b \\ \dot{v} &= a + b_{acc} + \eta_v \\ \dot{h} &= v + \eta_h\end{aligned}\quad (10)$$

which can be expressed in the state space formulation (11):

$$\dot{\mathbf{x}} = \mathbf{A}\mathbf{x} + \mathbf{B}\mathbf{u} + \boldsymbol{\eta} \quad (11)$$

with the \mathbf{A} , \mathbf{B} and \mathbf{Q} matrices of the form (12):

$$\mathbf{A} = \begin{pmatrix} 0 & 0 & 0 \\ 1 & 0 & 0 \\ 0 & 1 & 0 \end{pmatrix} \quad \mathbf{B} = \begin{pmatrix} 0 \\ 1 \\ 0 \end{pmatrix} \quad (12)$$

and state vector and input vector (13):

$$\mathbf{x}^T = [b_{acc}, v, h] \quad \mathbf{u} = [a] \quad (13)$$

Where h is the altitude of the platform, v is vertical speed and b_{acc} is the accelerometer bias. a is a linear acceleration along VTOL z-axis. Accelerometer bias is modeled as a random walk process. Process noise components η have zero mean and covariance matrix \mathbf{Q}

To obtain discrete Kalman Filter, we have to use discrete formulation of the system. For the discretization of the state equations first order approximation will be used (15):

$$\mathbf{x}(k+1) \approx (\mathbf{I} + \mathbf{A}T_s)\mathbf{x}(k) + T_s\mathbf{B}\mathbf{u}(k) + T_s\boldsymbol{\eta}(k) \quad (14)$$

$$= \boldsymbol{\Gamma}\mathbf{x}(k) + \boldsymbol{\Psi}\mathbf{u}(k) + T_s\boldsymbol{\eta}(k) \quad (15)$$

We assume that $\boldsymbol{\eta}(k)$ is white Gaussian with zero mean and unknown covariance matrix \mathbf{Q}_d . Discretization of equations (10) results in the discrete system with matrices (16).

$$\boldsymbol{\Gamma} = \begin{pmatrix} 1 & 0 & 0 \\ T_s & 1 & 0 \\ 0 & T_s & 1 \end{pmatrix} \quad \boldsymbol{\Psi} = \begin{pmatrix} 0 \\ T_s \\ 0 \end{pmatrix} \quad (16)$$

Measurement model is represented by discrete state space equation (17) and matrix (18), $\mu(k)$ is the measurement noise with covariance matrix R .

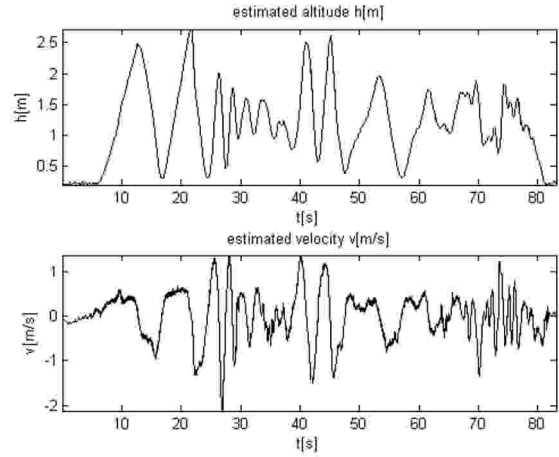


Fig. 3. State estimates during the identification experiment

$$y(k+1) = \mathbf{H}\mathbf{x}(k) + \mu(k) \quad (17)$$

$$\mathbf{H} = \begin{pmatrix} 0 & 0 & 1 \end{pmatrix} \quad (18)$$

In order to measure a accelerometer will be used, altitude information will be obtained from previously filtered ultrasonic measurement. For altitude, vertical velocity estimation discrete Kalman Filter described by the equations (19) is used.

$$\begin{aligned}\hat{\mathbf{x}}_{k|k-1} &= \boldsymbol{\Gamma}\hat{\mathbf{x}}_{k-1|k-1} + \boldsymbol{\Psi}\mathbf{u}_{k-1} \\ \mathbf{P}_{k|k-1} &= \boldsymbol{\Gamma}\mathbf{P}_{k-1|k-1}\boldsymbol{\Gamma}^T + \mathbf{Q}_d \\ \mathbf{e}_k &= \mathbf{z}_k - \mathbf{H}\hat{\mathbf{x}}_{k|k-1} \\ \mathbf{S}_k &= \mathbf{H}\mathbf{P}_{k|k-1}\mathbf{H}^T + \mathbf{R} \\ \mathbf{K}_k &= \mathbf{P}_{k|k-1}\mathbf{H}_k^T\mathbf{S}_k^{-1} \\ \hat{\mathbf{x}}_{k|k} &= \hat{\mathbf{x}}_{k|k-1} + \mathbf{K}_k\mathbf{e} \\ \mathbf{P}_{k|k} &= (\mathbf{I} - \mathbf{K}_k\mathbf{H})\mathbf{P}_{k|k-1}\end{aligned} \quad (19)$$

Where $\hat{\mathbf{x}}_{k|k-1}$ is a priori estimate of the state vector, $\hat{\mathbf{x}}_{k|k}$ is a posteriori estimate, by $\mathbf{P}_{k|k-1}$ we denote a priori estimate covariance, a posteriori estimate covariance is denoted by $\mathbf{P}_{k|k}$. Matrix \mathbf{S}_k is residual covariance and \mathbf{K}_k is the Kalman gain.

Comprehensive discussion on Kalman Filtering techniques can be found in Crassidis (2011); Simon (2006). We will treat output of Kalman Filter, as our final estimate of altitude and vertical velocity.

3.5 State estimation results

In a process of identification, altitude and vertical velocity estimates will be used. These values will be based on a use of the discussed Kalman Filter and rate of change limiter.

On Figure 3 estimation results are shown, it was possible to attenuate pulse errors in the ultrasonic measurements and to estimate vertical velocity which is free of the bias component.

By obtaining estimates of the vertical speed and altitude, it becomes possible to use these information sources in identification process.

4. IDENTIFICATION OF VERTICAL MOVEMENT MODEL

The knowledge about the controlled system gives a possibility to obtain the high performance control indices. The most common approach to explain how the plant is functioning is to determine the mathematical model as presented in one of previous sections. However, such model is always derived with some simplifications which can have an effect on neglecting some other dynamics, crucial in the control process. The other way to acquire the model of the dynamical system includes the design of experiments that consist in object excitation and outputs measurement. If the plant is stable one can perform the identification experiment in the open loop. For the quadrotor platform the following experiment has been planned. Operator of the platform changes the power of the motors using throttle stick from the RC apparatus, keeping in mind not to tilt in pitch and roll. The height and vertical velocity measurements are recorded. As an input to the model the collective thrust is given. The excitation signal should be sufficient enough to stimulate the identified system but some abrupt changes of the throttle stick can cause damage to the platform.

Phenomenological model of the quadrotor indicates that the system is nonlinear. Mainly the nonlinearities come from the motor units and body aerodynamics, thus to obtain a suitable model for the control strategy design purpose the class of nonlinear block-oriented model has been chosen. The models consist of linear dynamic blocks and nonlinear static blocks. When a nonlinear block precedes and follows a linear dynamic system the model is called a Hammerstein-Wiener Khalil and Yesildirek (2010) model. Considering the control possibilities two models are introduced for the explanation of vertical movement of the quad thrust aerial robot.

First model has been identified from the throttle to the velocity and it includes the nonlinearities. In Figure 4 the identification results have been presented. The Hammerstein-Wiener model, which describes the dynamics from motor control signal to the vertical velocity has the following form: 3 degree polynomial as an input nonlinearity (Figure 5) and piecewise continuous function with one unit as an output nonlinearity (Figure 6). The linear dynamic is provided as an output error model in the form depicted below 20:

$$G_1(z^{-1}) = \frac{V(z^{-1})}{U(z^{-1})} = \frac{-1.574z^{-3} + 0.572z^{-4} + z^{-5}}{1 - 1.801z^{-1} - 0.059z^{-2} + 1.525z^{-3} - 0.665z^{-4}} \quad (20)$$

The second model has been identified as an ARX parametric model. Normally height is an integral of the velocity, however the dynamic relation between those two signals has been modelled as a parametric model in the following form of the discrete transfer function 21 which is exactly an unstable pole, very close to the unity (integration action):

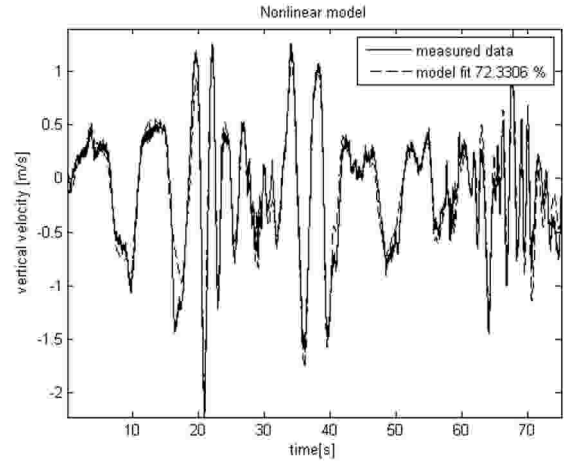


Fig. 4. Identification results of vertical speed model

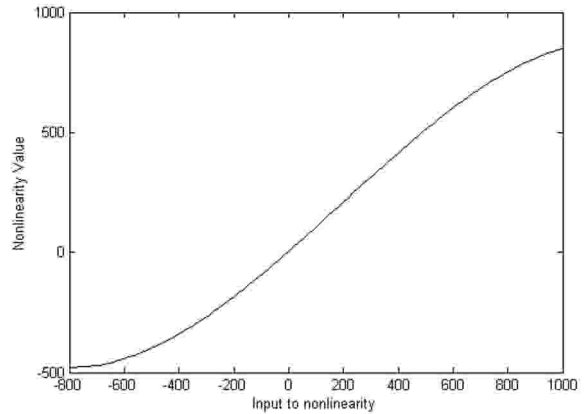


Fig. 5. Input nonlinearity

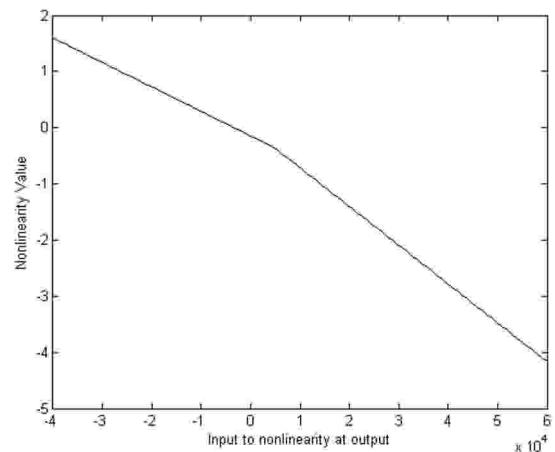


Fig. 6. Output nonlinearity

$$G_2(z^{-1}) = \frac{H(z^{-1})}{U(z^{-1})} = \frac{0.02131z^{-1}}{1 - 1.001z^{-1}} \quad (21)$$

In the figure 7 the result of comparison between the measured data and the model is presented.

The verification process conducted on the other set of data gives the proof that both structures of the models which

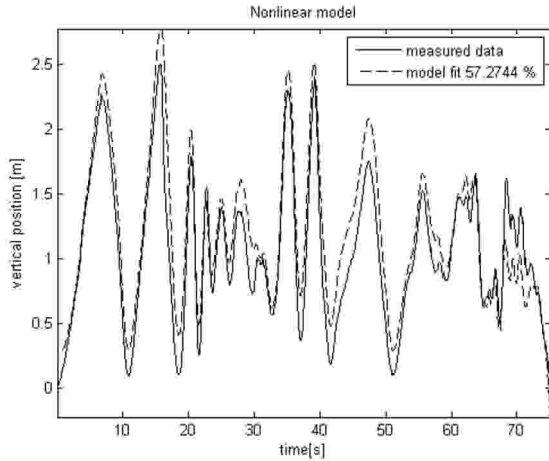


Fig. 7. Identification results of altitude model

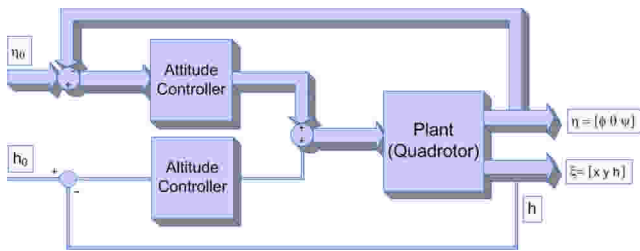


Fig. 8. General VTOL control scheme

have been previously selected seems to be sufficient enough for the control strategy design.

5. VERTICAL MOVEMENT CONTROL SCHEME

A general scheme of control system (8) consists of two subsystems: attitude stabilization around hovering conditions and altitude regulation. Both of control systems were designed based on the PID algorithm, but between them exists sufficient time-scale separation. It is achieved through proper selection of controller parameters.

The detailed description of the attitude stabilization, including various solutions, was presented in Czyba (2009) and Czyba and Szafranski (2013) In the next chapter, we will focus on the problem of altitude control.

5.1 Structure of altitude control system

The main task of the altitude control system is to achieve and remain in a desired position calculated along the z-axis direction. The reference value can be either the constant level above the ground or a trajectory defined for take-off and landing manoeuvres. The idea consists in data fusion from the different sensors, namely ultrasonic range finder and accelerometer. To estimate the height of flight and velocity in vertical motion, the Kalman filter was applied (section 3).

During precise maneuvers, such as taking-off and landing, the high accuracy in the altitude control is required. Taking this into account, the cascade control system was applied (Fig. 9).

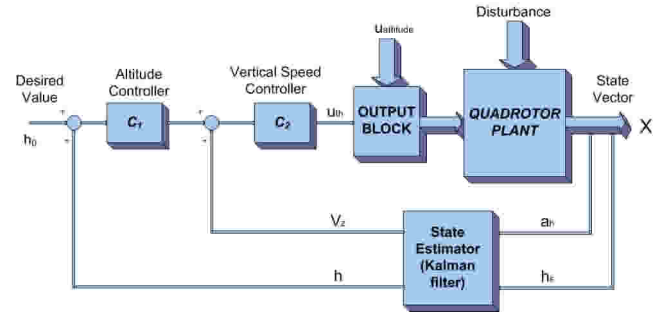


Fig. 9. Implemented altitude control scheme

Basically, in a cascade control schema the plant has two or more outputs. This requires an additional sensor to be employed so that the fast dynamics can be measured. The primary controller and the primary dynamics are components of the outer loop. The inner loop is also a part of the outer loop, since the primary controller calculates the set point for the secondary controller loop. Furthermore, the inner loop represents the fast dynamics, whereas the outer should be significantly slower (with respect to the inner loop). This assumption allows interaction that can occur between the loops to be restrained, improving stability. Therefore, a higher gain in the inner loop can be adopted. An additional advantage is that the plant nonlinearities are handled by the controller in the inner loop, and exert no meaningful influence on the outer loop (Visioli (2006), Wade (2004)). In this work the cascade control structure is proposed as a solution to control tasks formulated as altitude regulation. The vertical speed is estimated by the Kalman filter and can be used in the inner loop. The outer loop is based on the altitude estimated also by the Kalman filter as a result of data fusion from used sensors: ultrasonic range finder and accelerometer. Both controllers were designed based on the PID algorithm, and parameters were tuned using the identified quadrotor model in vertical flight. The control signal from cascade controller is combined together with attitude controller to generate the control inputs through , for motors 1 to 4. The main goal of the output block is to accomplish an algorithm of quadrotor control, and provides decoupling of control channels in steady state.

5.2 Tests and results

In this section, we present the results of simulations which was conducted to evaluate the performance of the designed altitude control system in the cascade structure with PD controller in the inner loop and P controller in outer loop. The presented simulations consisted in transition from one steadystate flight to another with respect to the reference value (step or ramp). To evaluate the quality of control the comparison between the simulated and the real control system has been presented (Figure 10).

The simulations in Matlab/Simulink environment and tests on the real plant were performed for the same structure of control system (Figure 9) and the same values of controller parameters. The variations of process variable from the real plant are due to the longitudinal and lateral motions, which are inevitable in the real flight. In simulations there are no interaction between attitude and altitude control loops, because the motion analysis

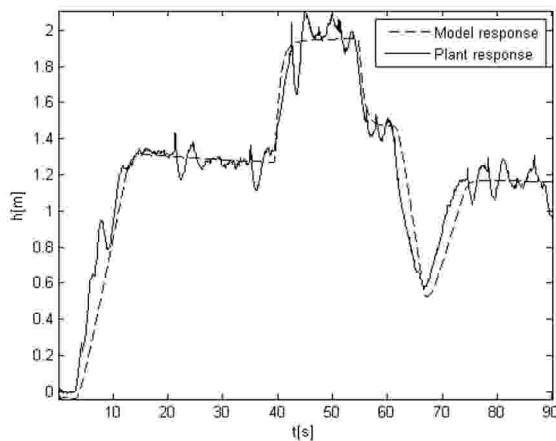


Fig. 10. Comparison of the closed loop system responses, for identified model and a real plant

has been only considered in vertical axis. The results which have been obtained confirm the correctness of the performed identification process, and allows to conclude that identified model is satisfactory enough in terms of quality. Some discrepancies between the results point at the high complexity of the flying platform dynamics in various states of flight such as hover, climb and descent.

6. CONCLUSIONS

In this paper, the problem of altitude control in scope of data processing, state estimation, and model identification has been presented. Considering the phenomenological model of quadrotor, which includes rigid body model, propulsion system and aerodynamics, the conclusions about the high complexity of its dynamics in various states of flight, especially of the vertical movement, can be made. Taking into account the above conclusions and model nonlinearities, the identification experiment of the quadrotor vertical motion has been performed. The nonlinear Hammerstein-Wiener model has been proposed as an approximation of different quadrotor states of flight. In view of the precise maneuvers in vertical flight and identification process, the estimation of vertical velocity and height of flight is required. On the basis of the ultrasonic range finder and accelerometer measurements, the Kalman filter was designed and also applied in the quadrotor autopilot hardware. For high accuracy in the altitude control, the controllers in the cascade structure has been implemented. The parameters of the controllers have been tuned using the model obtained during the identification experiments. Finally, the designed control system has been successfully transferred to the quadrotor hardware unit and tested under the real operating conditions.

ACKNOWLEDGEMENTS

This work has been partially granted by the Polish Ministry of Science and Higher Education from funds for years 2012-2013.

The authors Wojciech Janusz and Grzegorz Szafranski are scholars from the "DoktorIS - Scholarship Program for Silesian Innovation" co-funded by the European Union from the European Social Fund.

REFERENCES

- Bouabdallah, S., Noth, A., and Siegwart, R. (2004). Pid vs lq control techniques applied to an indoor micro quadrotor. In *Intelligent Robots and Systems, 2004. (IROS 2004). Proceedings. 2004 IEEE/RSJ International Conference on*, volume 3, 2451–2456 vol.3.
- Bouabdallah, S. (2007). *Design and control of quadrotors with application to autonomous flying*. Ph.D. thesis, Lausanne.
- Bristeau, F. Callou, D., and Vissiere (2011). The navigation and control technology inside the ar.drone micro uav. In *Preprints of the 18th IFAC World Congress*, 1477–1484.
- Castillo, P., Lozano, R., and Dzul, A.E. (2005). Modelling and control of mini-helicopters. In *Modelling and Control of Mini-Flying Machines*, Advances in Industrial Control, 81–119. Springer London.
- Crassidis, J.L, J.J. (2011). *Optimal Estimation of Dynamic Systems*. Chapman and Hall/CRC, London.
- Czyba, R. (2009). Design of attitude control system for an uav type-quadrotor based on dynamic contraction method. In *Proc. of IEEE/ASME International Conference on Advanced Intelligent Mechatronics*.
- Czyba, R. and Szafranski, G. (2013). Control structure impact on the flying performance of the multi-rotor vtol platform - design, analysis and experimental validation. *International Journal of Advanced Robotic Systems*.
- Khalil, B. and Yesildirek, A. (2010). System identification of uav under an autopilot trajectory using arx and hammerstein-wiener methods. In *Mechatronics and its Applications (ISMA), 2010 7th International Symposium on*, 1–5.
- Leishman, J. (2006). *Principles of Helicopter Aerodynamics. 2nd ed.* Cambridge University Press, New York.
- Nonami, K., Kendoul, F., Suzuki, S., Wang, W., and Nakzawa, D. (2010). *Autonomous Flying Robots*. Springer, London.
- Seddon, J. (1990). *Basic Helicopter Aerodynamics*. British Library.
- Simon, D. (2006). *Optimal State Estimation: Kalman, H Infinity, and Nonlinear Approaches*. Wiley-Interscience.
- Szafranski, G., Czyba, R., Janusz, W., and Blotnicki, W. (2013). Altitude estimation for the uav's applications based on sensors fusion algorithm. In *Unmanned Aircraft Systems (ICUAS), 2013 International Conference on*, 508–515. doi:10.1109/ICUAS.2013.6564727.
- Tayebi, A. and McGilvray, S. (2006). Attitude stabilization of a vtol quadrotor aircraft. *Control Systems Technology, IEEE Transactions on*, 14(3), 562–571.
- Valavanis, K. (2007). *Advances in Unmanned Aerial Vehicles*. Springer-Verlag, Dordrecht.
- Visioli, A. (2006). *Practical PID Control*. Springer-Verlag, London.
- Wade, H. (2004). *Basic and Advanced Regulatory Control: System Design and Application*. ISA, United States of America.